

AIP CONFERENCE PROCEEDINGS 288

LASER ABLATION: MECHANISMS AND APPLICATIONS-II SECOND INTERNATIONAL CONFERENCE KNOXVILLE, TN APRIL 1993

EDITORS:

JOHN C. MILLER
DAVID B. GEOHEGAN
SOLID STATE DIVISION
OAK RIDGE NATIONAL
LABORATORY

**AIP
PRESS**

American Institute of Physics

New York

Authorization to photocopy items for internal or personal use, beyond the free copying permitted under the 1978 U.S. Copyright Law (see statement below), is granted by the American Institute of Physics for users registered with the Copyright Clearance Center (CCC) Transactional Reporting Service, provided that the base fee of \$2.00 per copy is paid directly to CCC, 27 Congress St., Salem, MA 01970. For those organizations that have been granted a photocopy license by CCC, a separate system of payment has been arranged. The fee code for users of the Transactional Reporting Service is: 0094-243X/87 \$2.00.

© 1994 American Institute of Physics.

Individual readers of this volume and nonprofit libraries, acting for them, are permitted to make fair use of the material in it, such as copying an article for use in teaching or research. Permission is granted to quote from this volume in scientific work with the customary acknowledgment of the source. To reprint a figure, table, or other excerpt requires the consent of one of the original authors and notification to AIP. Republication or systematic or multiple reproduction of any material in this volume is permitted only under license from AIP. Address inquiries to Series Editor, AIP Conference Proceedings, AIP Press, American Institute of Physics, 500 Sunnyside Boulevard, Woodbury, NY 11797-2999.

L.C. Catalog Card No. 93-73040
ISBN 1-56396-226-8
DOE CONF-9304144

Printed in the United States of America.

**Extending Laser Fusion Concepts Into the Lower Power
($\lesssim 1 \text{ GW/cm}^2$) Microelectronics Arena.**

Russell W. DREYFUS
IBM Research Div., TJ Watson Research Center
P.O. Box 218, Yorktown Heights, NY 10598 USA

Claude PHIPPS
Chemical and Laser Science Div., Los Alamos National Lab.
Los Alamos, NM 87545 USA

Akos VERTES
Chemistry Dept., George Washington Univ.
Washington D.C. 20052 USA

Analysis of high power ($I \gtrsim 10^{11} \text{ W/cm}^2$), short pulse ($\tau \sim 10 \text{ ns}$) surface ablation has existed for years. This talk provides a summary of extending the analysis into the lower power levels, $\lesssim 10^9 \text{ W/cm}^2$, characteristic of excimer laser machining in the microelectronics range of power densities. As is generally known, the result is the formation of a dense ($> 10^{19} \text{ cm}^{-3}$), thin ($\gtrsim 30 \mu\text{m}$) surface plasma due to optical absorption by free electrons. We compare these results to the nanosecond changes in densities and temperatures as determined by computer modeling. Modeling of copper colliding with a background gas indicates the importance of the "snowplow" buildup on the leading edge of the expanding gas cloud, and complements LIF measurements on copper reoxidation in O_2 and N_2O atmospheres. Also the modeling provides results for the surface overpressure. Commonly, we see surface pressures in the > 100 atmosphere range. The rebound (cavitation bubbles) from such transient pressures are one source of particulates from molten surfaces; i.e. debris. This is in agreement with the bursting of these bubbles producing the regions of observed locally coherent surface waves.

I. Introduction

UV excimer lasers are expanding their applications in the areas of material etching and pulsed laser-induced deposition, PLD. The usual irradiance, I , is in the $\lesssim 500 \text{ MW/cm}^2$ for reasons of efficiency, minimizing unwanted chemical decomposition, and thermal or pressure complications. The fact that these irradiations fall into a region of essentially one dimensional (1D) effects due to the moderately short pulse length, $\tau \sim 10 \text{ ns}$, and short wavelength, $\lambda \sim 248 \text{ nm}$, means that simple analytic models adequately describe the physics of the situation. Furthermore, the present tendency to utilize homogeneous irradiations, rather than Gaussian beam profiles, contributes to easier interpretation of both the experimental and modeling results. While significant modeling was described in the early days of laser etching, much of the emphasis was on values of I , λ , and τ , much larger than the present range. Thus it is again useful to look closely at this region of microelectronic interest near $\lesssim 0.5 \text{ GW/cm}^2$.

II. Modeling

The primary assumptions in modeling the laser ablation are: a 1D geometry, local thermodynamic equilibrium, and heating of the free electrons in the plume by inverse bremsstrahlung, IB. The results from these assumptions will be presented starting at reasonably high energies (10^{15} to 5×10^8 W/cm²), and then connected with a computer cell model. Lastly, the results will be used to obtain insight into snowplow reactions of Cu with oxygen and, to the effects of surface gas pressures and surface motion on surface splashing and debris formation.

An analytical model has been described in detail in Ref. 1. The principal assumption is that the above surface plasma is sufficient to transmit only e^{-1} of the incident ablation energy down to the surface. It need not be specified whether the transmission is due to a less than completely opaque plasma or energy relaying by radiation or plasma thermal conductivity. While it was originally shown that $I \gtrsim 1$ GW/cm² in the UV is sufficient for validity, the present work will show that slightly less, i. e. 500 MW/cm², results in quite similar relationships and concepts.

Reference 1 may be used to predict many of the interesting ablation parameters with good accuracy over a broad range of laser wavelengths (0.25 to 10 μ m), and pulse durations (up to 1 ms).

$$\text{Pressure: } p_a = 5.83 \frac{\Psi^{9/16}}{A^{1/8}} \frac{I^{3/4}}{(\lambda\sqrt{\tau})^{1/4}} = 21.4(I^3/\lambda\sqrt{\tau})^{1/4} \text{ dynes/cm}^2 \quad (1)$$

(10^6 dynes/cm² = 1 bar \sim 1 atmosphere pressure).

$$\text{Temperature: } T_e = 2.98 \times 10^4 \frac{A^{1/8} Z^{3/4}}{(Z+1)^{5/8}} (I\lambda\sqrt{\tau})^{1/2} \text{ K} = 2.8(I\lambda\sqrt{\tau})^{1/2} \text{ eV} \quad (2)$$

$$\text{Plume density: } n_e = 3.6 \times 10^{11} \frac{A^{5/16}}{Z^{1/8}(Z+1)^{9/16}} \frac{I^{1/4}}{(\lambda\sqrt{\tau})^{3/4}} = 9 \times 10^{11} \frac{I^{1/4}}{(\lambda\sqrt{\tau})^{3/4}} \text{ cm}^{-3} \quad (3)$$

$$\text{Ablation rate: } \dot{m} = 2.66 \frac{\Psi^{9/8} I^{1/2}}{A^{1/4} \lambda^{1/2} \tau^{1/4}} = 35.79(I/\lambda\sqrt{\tau})^{1/2} \mu\text{g/cm}^2\text{s} \quad (4)$$

which for copper can be expressed as an ablation depth of $40(I\tau^{1.5}/\lambda)^{1/2}$ nm

$$\text{Velocity: } c_{\text{plume}} = 1.37 \frac{A^{1/8}}{\Psi^{9/16}} (I\lambda\sqrt{\tau})^{1/4} \text{ cm}/\mu\text{s} = 0.37(I\lambda\sqrt{\tau})^{1/4} \text{ cm}/\mu\text{s} \quad (5)$$

where I is in W/cm²; λ is in cm, and τ in seconds.

$$\text{The parameter } \Psi = \frac{A}{2[Z^2(Z+1)]^{1/3}}$$

where A is the atomic mass and Z is the charge state of the ion. The values on the right above are for copper (singly ionized at most), but which depend only weakly on material properties. One significant change is that the escape velocity for ions should be 2.5 times higher than c_{plume} due to the coulombic acceleration in the outer plasma layer.¹ This, of course, translates into a > 6 times higher kinetic energy, but is often moderated by resonant charge exchange collisions in the expanding plume.

The results of the above relations are both interesting and self consistent. The product of the temperature times density, etc. indicate that 1/3 of the energy is in the *c.m.* flow of the plume cloud, 1/3 is in the *internal energy* of the cloud, and $\sim 1/3$ is *lost to the surface*.

The internal energy of the cloud is the source of x-ray energy, which is useful for short wavelength lithography. Since radiative cooling is dominant for the plume, one need only estimate the percentage of radiation in the desired wavelength range, and in the time interval before "freezing in" the electron temperature to obtain an estimate of the x-ray output.

III. Transition to a Transparent Plume

The model described in Ref. 2 bridges to irradiances below those covered above. This is useful since for $I < 500$ MW/cm², as the plume is transparent and the Phipps model¹ no longer applies. This Vertes model² is based on classical thermodynamic quantities (including temperature dependences where applicable) plus the IB cross section.

A result for $I = 500$ MW/cm² is illustrated in Fig. 1. Results from such calculations are in quite reasonable agreement with the expressions, (1) to (5), of Phipps. For instance, the latter gives $T_e = 3.74$ eV, while Ref. 2 gives some double ionization with $T_e \sim 10$ eV but a vast majority of the plume is at 3 to 4eV, see Fig. 1. There exists experimental values³ for T_e of 1.5eV, although this is after a flight path of 10 cm. Also Eq. (3) gives a plume density $n_e = 2.9 \times 10^{20}$ cm⁻³, while Fig. 1 shows $10^{20} < n_e < 3 \times 10^{20}$ cm⁻³. The connection between analytical modeling¹ and a computer model² of cells, thermodynamics, etc. thus connects up smoothly at $I \gtrsim 500$ MW/cm². Furthermore, an experimental value³ is $\sim 6 \times 10^{19}$ Cu/cm³ as extracted from the *ion* density at 10 cm (neutral Cu⁰ is not counted by the Langmuir probe measurements³). While suggesting some recombination and cooling, the latter measurement still leaves the densities and energies near the original sub-microsecond values.

At $I < 500$ MW/cm², the model of Ref. 1 is no longer applicable as the plume is not opaque and $\gg 1/3$ the incident flux reaches the "solid" surface. Simple techniques for estimating the inverse bremsstrahlung cross section, σ_{IB} , clarify why this transition to a semitransparent plume occur in the present fluence range.

In the UV, σ_{IB} depends primarily on the (dephasing) scattering frequency, ν_e , for free electrons, e.g.

$$\sigma_{IB} = \frac{\alpha}{n_e} \sim \frac{\nu_e \nu_p^2}{c \nu^2 n_e} \sim \pi^{-1} 10^{-23} \lambda^2 \cdot \nu_e \text{ cm}^2 \quad (6)$$

where ν and λ pertain to the ablation laser. Eq. (6) is under the presumption that $\hbar\omega < 2kT_e$; when this is not correct (6) is reduced by the above factor, typically 2 to 5. Effectively, (6) is the Lorentzian tail of an infrared plasma frequency (extending into the UV). With neutral Cu densities of 3×10^{20} cm⁻³ and assuming an (energy independent) Cu⁰ scattering cross section of 50 \AA^2 , one finds⁴ $\sigma_{IB} \sim 2.5 \times 10^{-20}$ cm⁻² for the scattering due to *neutral* species. The critical question is when does sufficient electron heating occur to bring the temperature above the Cu surface, $T_s \sim 5000\text{K} \sim 0.4\text{eV}$, and instead bring it into the ionizing range of $T_e \sim 2$ eV. Two points must be quantitatively followed. First, ν_e depends on $T_e^{-1.5}$, so that for T_e as low as 0.4eV the scattering cross section due to *ions* gives a very large σ_{IB} , e.g. 0.5 to 1×10^{-19} cm². With an incoming flux of

8×10^{18} photons/cm², one sees that the electrons typically absorb about one photon. Under the assumption of local thermal equilibrium, this extra energy would first act to exponentially increase both the free electron and ion density. For instance, an increase of T from 4000K to 6000K in the plume would then increase $n_e > 10 \times$. This increase in n_e is felt as an increase in the ν_e scattering frequency, and hence σ_{IB} which means that the electron cloud rapidly becomes predominantly ionized by run away electron heating (into the ~ 2 eV range).

The principal point of the above consideration is that electron scattering requires a combination of neutral density of $\sim 3 \times 10^{20}$ cm³ along with a low T_e for breakdown (thermal runaway) with 500 MW/cm² $\sim 8 \times 10^{18}$ photons/cm². The critical quantity in the plasma breakdown in other materials is the question of the minimum fluence required to produce an electron scattering rate $\gtrsim 10^{14}$ s⁻¹. Secondary changes in the breakdown threshold are brought about by such questions as the laser fluence required to promote this scattering rate (polymers ablate at ~ 10 MW/cm² so plasma formation is not required, but may occur at sufficient intensity). Returning to Cu, it is clear that no plasma breakdown occurs with 100 MW/cm² as the plume density is only $\sim 10^{16}$ Cu^o/cm³ and ν_e is orders of magnitude too small to produce electron heating.²

Figure 2 shows the effect of plasma formation on the surface temperature at the end of the 10ns pulse. With 250 MW/cm² virtually no plasma breakdown is predicted, hence T_s has just been rising as $t^{1/2}$. In the other extreme of 1.1 GW/cm², the plasma is so dense after ~ 1 ns that the surface starts to cool due to shadowing. As detailed above, 500 MW/cm² is essentially on the threshold, which now appears to set in slowly, i.e. at ~ 6 ns. This onset is at the point where the initial $t^{1/2}$ rise changes (in going from $t = 6 \rightarrow 8$ ns) into surface shadowing. The etch laser energy is thus now deposited in the plume producing the results of Fig. 1 — a highly heated plasma over a moderately hot surface, $T_s \sim 4000$ K.

IV. Applications of the Model

Besides giving insight into the plasma formation process, the modeling is useful for clarifying several other points. First, consider that most pulsed laser depositions, PLD, are carried out at 248nm with 2 to 4J/cm²; i.e. 200 to 500 MW/cm². This fluence is just below the range which usually forms an intense plasma. One now can see how this point was arrived at empirically as it avoids both dissociation of complex oxides, e.g. in high temperature superconductors, HTSC, and wasting energy by depositing it in the plume instead of on the surface. Under the usual condition that the total laser energy is limited, Eq. (4) shows that the maximum material is transferred when I is minimized by spreading the energy over a "large" area. The only limitation is that one wishes to be on the brink of intense plasma formation which parallels the maximum T_s , see Fig. 2 in order to elevate the vapor pressure.

Second, one can follow the reoxidation of Cu for HTSC. The reaction $\text{Cu} + \text{O}_2 \rightarrow \text{CuO} + \text{O}$ is highly (~ 2.3 eV) endothermic. Actually, it appears that the O_2 dissociation occurs on the snowplow front due to compressional heating. We have observed that the reaction occurs slowly, 30 to 100 μ s for it to be a direct collisional reaction. Part of the reason is that while the Cu is travelling at 5 to 10 eV in the laboratory, in the center-of-mass frame the relative Cu and O collision occurs at ~ 4 eV. This energy is barely over threshold hence does not present a large cross section. Sec-

ond, when one calculates the interdiffusion of O into the dense Cu clouds using present plume densities one finds that many microseconds are required.

A last interesting point is to look at the formation of debris; i.e. μm sized particulates. Their presence is one of the serious detractors to PLD. Figure 3 illustrates that there is a significant gas pressure on the surface even when ablating $<< \mu\text{m}^2$; i. e. 150 nm from Eq. (4). The important point is that while $p > 100$ bar (Eq. (1)), it is nevertheless relieved in a few nanoseconds. During the ablation pulse, the surface has been compressed ($\sim 0.1\%$) down to a depth of $\sim 50\mu\text{m}$ as given by the speed of sound in solid Cu. The rapid ($\lesssim 2$ ns) relief of this pressure will give an outward acceleration. Presuming that nearly linear mechanical properties apply, the result would be a negative pressure on the next half cycle of surface "bounce". In the original model and not yet incorporating surface motion, the thermal behavior of Cu effectively couple T_s to the Cu vapor pressure. This occurs as a result of two factors, i.e. heat of vaporization is a major source of surface cooling, and the high thermal conductivity of Cu prohibit subsurface temperatures higher than T_s . The pressure relief cycles after the 10ns pulse appear to break the above limitation on pressure. As the surface first accelerates and ~ 20 ns later decelerates (involving stresses $\gtrsim 100$ bar) the outer surface layers will be under tensile stress.⁵ In the top $\sim 1/2 \mu$ of liquid Cu this will cause boiling or equivalently cavitation. As these bubbles reach the surface and break they both throw off debris droplets and cause the locally parallel wavelets reported by Kelly *et al.*⁶ This is somewhat different than the well known sidewise "squirting" one sees with $>> \mu\text{s}$ pulses.⁷

In summary, one can readily utilize quantitative models to explain a number of features, e.g. plasma formation, oxidation reactions and overpressure effects. In doing so, significant (semiquantitative) insight is obtained.

References

1. C. Phipps and R. W. Dreyfus, *Bull. Amer. Phys. Soc.* **37**, 83 (1992); "Laser Ablation and Plasma Formation", C. R. Phipps and R. W. Dreyfus, book chapter in *Laser Ionization Mass Analysis*, ed. by A. K. Vertes, R. Gijbels and F. Adams, John Wiley and Sons Publishers, (New York, NY), in press; and C. R. Phipps, T. P. Turner, R. F. Harrison, G. W. York, W. Z. Osborne, G. K. Anderson, X. F. Corlis, L. C. Haynes, H. S. Steele, and K. C. Spicochi, *J. Appl. Phys.* **64**, 1083 (1988) and the references therein.
2. A. Vertes, this conference, and A. Vertes, D. Platt and R. Dreyfus, *IBM J. of Res. and Dev.*, to be published, and A. Vertes, P. Juhasz, M. De Wolf and R. Gijbels, *Scanning Microscopy* **2**, 1853 (1988), and *J. Mass Spec. and Ion Processes*, **94**, 63 (1989) and the references therein.
3. R. von Gutfeld and R. Dreyfus, *Appl. Phys. Lett.* **54**, 1212 (1989).
4. R. W. Dreyfus, *Surface Science*, edited by Profs. K. Terakura and Y. Murata, (Springer-Verlag, Berlin), v. **283**, 177 (1993).
5. A. Oraevsky, *Dynamical Response of Materials to Pulsed Heating Workshop*, Los Alamos National Lab. and S.D.I.O., 23 Jan 1993.
6. R. Kelly *et al.*, *Nucl. Instru. and Meth.*, **B9**, 329 (1985).
7. J. von Allman, *J. Appl. Phys.* **47**, 5460 (1976), and Broer and Vriens, *Appl. Phys.* **A32**, 107 (1983), and S. Goldman *et al* *SPIE* **1279**, 2 (1990).

Fig. 1 Sample result from Ref. 2 for 500 MW/cm² and at the end of the 10ns pulse. The plume is primarily at a density of $\sim 2.5 \times 10^{20}$ Cu/cm³ and singly ionized; however, there exists a small region near 12 μ m that is doubly ionized.

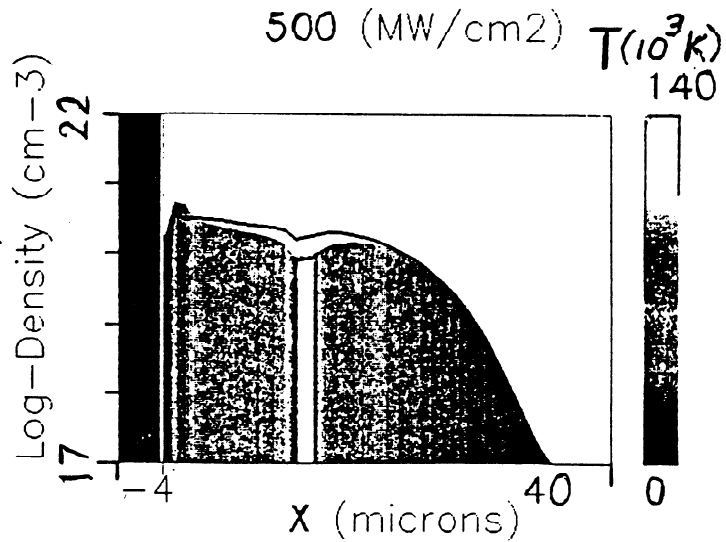


Fig. 2 Surface temperature, T_s , as a function of time during a 10ns pulse. Note that the (above surface) plasma becoming opaque is evidenced by surface cooling before the ends of the 0.5 and 1.1 GW/cm² pulses. On the other hand, the 250 MW/cm² pulse does not avalanche within the present 10ns pulse, hence surface shadowing is avoided.

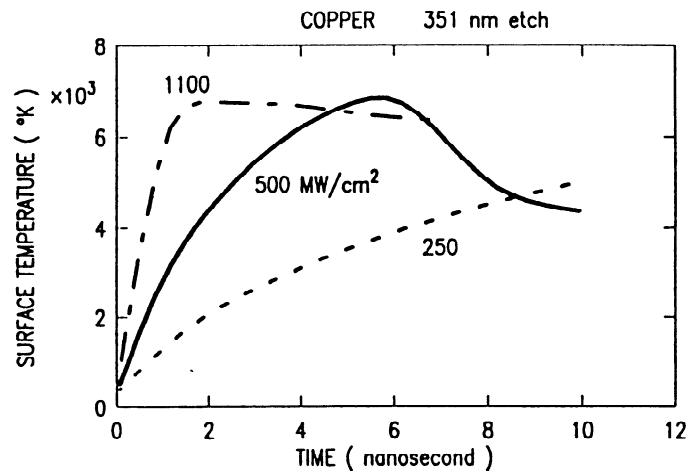


Fig. 3 Surface pressure vs. t for a "top-hat" and "exponential" pulse shape, both with 2.5 J/cm². In both cases, very high surface pressures exist for several nanoseconds, which are rapidly relieved. It is in this relief cycle that cavitation is presumed to occur.

